Contemporary Mathematics
https://ojs.wiserpub.com/index.php/CM/

Research Article

Numerical Solutions of Time-Fractional N-W-S and Burger's Equations Using the Tarig Projected Differential Transform Method (TPDTM)

Athira K[1], Narsimhulu D[1*], P. S. Brahmanandam[2]

[1] Department of Statistics and Applied Mathematics, Central University of Tamil Nadu, Neelakudi, Thiruvarur, 610005, Tamil Nadu, India
[2] Department of Physics and R & D Cell, Shri Vishnu Engineering College for Women (A), Vishnupur, Bhimavaram, 534202, India
E-mail: narsimha.maths@gmail.com

Received: 11 December 2024; **Revised:** 11 February 2025; **Accepted:** 11 March 2025

Abstract: Solving time-fractional nonlinear equations, such as the Newell-Whitehead-Segel (N-W-S) and Burger's equations, is inherently complex due to the intricacies of fractional calculus and the limitations of current numerical and analytical techniques. This study introduces the Tarig Projected Differential Transform Method (TPDTM), a hybrid approach that offers a novel solution to time-fractional linear and nonlinear partial differential equations (PDEs) without the need for linearization, perturbation, or variable discretization. TPDTM stands out as a simple yet powerful method, offering remarkable accuracy, computational efficiency, and ease of implementation. In comparative analysis with the Finite Difference Method (FDM) and Laplace Adomian Decomposition Method (LADM), TPDTM demonstrates superior performance, particularly in its handling of Adomian polynomials, all while preserving stability and precision. With its rapid convergence and versatility, TPDTM proves to be a robust tool for tackling complex fractional PDEs, making it highly valuable for applied mathematics and physics. Looking forward, expanding TPDTM's application to coupled fractional systems and multi-scale problems will not only enhance its theoretical depth but also open exciting new possibilities for breakthroughs in engineering, physics, and computational modeling.

***Keywords*:** fractional calculus, tarig projected differential transform method, newell-whitehead-segel (N-W-S) and burger's equations, numerical approximate solution, applied mathematics and physics

MSC: 26A33, 65M12

1. Introduction

Fractional calculus, a fascinating extension of classical calculus, delves into the realm of arbitrary derivatives and integrals, redefining how we approach mathematical modelling. Unlike traditional integer-order derivatives, which operate locally, fractional-order derivatives possess a unique non-local characteristic, capturing memory effects and long-range dependencies. This non-locality makes fractional differential equations (FDEs) a powerful generalization of classical differential equations, bridging the gap between theory and real-world complexities. While many conventional models rely on integer-order derivatives, they often struggle to fully capture the intricacies of nonlinear systems. FDEs, on the other hand, provide a more flexible and accurate framework, making them indispensable in modern scientific and engineering applications.

DOI: https://doi.org/10.37256/cm.6320256239

From signal and image processing to control systems, vibration analysis [1], biomedical engineering [2], fluid mechanics [3], and chemistry [4], fractional calculus have transformed the way we simulate and analyze complex processes. By incorporating memory and hereditary properties, fractional models offer deeper insights into dynamic behaviors that classical equations fail to address effectively. As research in this field continues to advance, its potential to revolutionize various disciplines grows exponentially, paving the way for more precise and efficient modeling of real-world phenomena.

The choice of a fractional derivative defines a system's mathematical structure and physical relevance, crucial for extending models to capture complex phenomena. Various definitions-Riemann-Liouville, Caputo, Caputo-Fabrizio, Grunwald-Letnikov, Riesz, and Atangana-Baleanu-address different modeling needs. The Caputo derivative suits physical systems with standard initial conditions, while Riemann-Liouville is mathematically rigorous but may introduce non-physical constraints. For processes with smooth memory effects, Atangana-Baleanu and Caputo-Fabrizio derivatives offer superior modeling. Each derivative also presents unique numerical challenges, influencing computational methods for solving fractional differential equations [5, 6].

Numerous strategies have emerged to solve differential equations involving fractional-order derivatives to attain more consistency and accuracy of the solution. Among the most sophisticated numerical techniques are the Adomian Decomposition Method (ADM) [7], the Homotopy Perturbation Method (HPM) [8], the Homotopy Perturbation Transform Method (HPTM) [9], the Laplace Decomposition Method (LDM) [10], the Finite Element Method (FEM) [11], FDM [12], the Variation Iteration Method (VIM) [13], the New Iterative Method (NIM) [14], LADM [15], the Perturbation Iteration Transform Method (PITM) [16], the New Homotopy Analysis Transform Method (NHATM) [17], and the Homotopy Analysis Method (HAM) [18].

Each of these approaches offers distinct advantages, yet none are without limitations. While FEM is powerful, particularly in handling complex geometries and boundary conditions, its efficacy diminishes when applied to large-scale three-dimensional (3D) problems. The accuracy of its solutions is highly contingent on mesh quality, and refining this mesh comes at a significant computational cost. Thus, despite their advancements, these methods still present challenges, paving the way for continued research into even more refined and efficient solutions.

HPM offers analytical approximations, but it may not be effective for non-linear systems. The major flaw of HPM is that it needs to calculate the functional equation for each iteration, a difficult and time-consuming. Both HPM and HPTM depend on building a suitable homotopy, which can be difficult for complicated problems and requires a balance between perturbation and iteration terms, which is not always intuitive. The LDM and FDM may have trouble guaranteeing convergence over a long-time interval. LADM is helpful for series solutions, but complex boundary conditions may cause it to fail to converge or necessitate considerable adjustments. Much effort has been put into developing the analytical and numerical solutions for a variety of linear and nonlinear fractional differential equations. For instance, the time-fractional Zakharov-Kuznetsov (ZKE) [19], Burgers-Huxley (BH) [20], Noyes-Field (NF) model of Belousov-Zhabotinsky (BZ) [21], Benjamin Bona Mahony Burger (BBMB) [22], Poisson (P) [23], Telegraph (TE), Laplace (L) and Wave (W) Equations [24].

In this research, we solve the time-fractional PDEs using a unique hybrid approach called the TPDTM [25], which combines the transform [26] with the Projected Differential Transform Method [27]. To understand the efficiency of this recently developed approach, we consider two distinct differential equations, namely the fractional N-W-S equation and Burger's equation. An attempt is made to compare hybrid TPDTM technique with well-known numerical methods, including FDM and LADM, respectively.

The standard N-W-S equation [28] of integer order is defined as follows

$$U_t = kU_{xx} + aU - bU^q.$$

where $U(x,\ t)$ is a function of space $(x \in R)$ and time $(t \geq 0)$ co-ordinate. Here, U represents the modelled physical quantity such as non-linear temperature distribution in either a narrow and infinitely long rod or the flow velocity of fluid in a pipe of small diameter and infinite length. The derivative, U_t represents the first order partial rate of change of U

with respect to time. The derivative U_{xx}, represents the second order partial rate of change in U with respect a given space variable (coordinate) x. Here, $k > 0$ is the diffusion coefficient, the term aU represents the linear source, $-bU^q$ represents the non-linear source term, and the exponent term q controlling the non-linear nature, and $q = 3$, is the standard value for the N-W-S equation [28].

In this work, we analyse the fractional model of the N-W-S equation of the form

$$D^{\alpha}U = kU_{xx} + aU - bU^q,\ 0 < \alpha \leq 1.$$

where the parameter α, which indicates the order of the time-fractional derivative. The fractional derivative has been taken in Caputo's sense. If $\alpha = 1$, the fractional N-W-S equations reduce to the classical N-W-S equation.

The time-fractional N-W-S equation models particle motion while incorporating memory effects. When variations exhibit heavy-tailed behaviour, a space-fractional derivative naturally emerges, capturing particle dynamics and the influence of low-field variations across the system. Furthermore, the fractional order in the temporal derivative indicates a weighted adjustment of system memory. As a result, a deep understanding of the time-fractional N-W-S equation is essential [28]. The well-known amplitude equation (the N-W-S equation) also explains the dynamic behavior of many physical systems close to their bifurcation point. It is a powerful tool for analyzing the binary fluid mixture's pattern formation and dynamics in Rayleigh-Benard convection [29] and pattern formation in reaction-diffusion systems [30]. This equation also captures the system's essential physics near the onset of instability several researchers have, therefore, applied various numerical techniques such as ADM [7], HPTM [9], FEM [11], NIM [14], VIM [28], LADM [31], and MRPSM [32] to find the approximate solution of the N-W-S equation.

A non-linear PDE-classical Burger's equation, is fascinating to researchers exploring a wide range of physical phenomena, including shock wave theory, fluid dynamics, turbulent flow, and gas dynamics [33, 34]. This equation is one of the most helpful equations for formulations of shock wave behavior, revealing non-linear advection and diffusion [33]. Bateman initially examined the Burger equation, which looks as follow.

$$U_t + UU_x = VU_{xx}.$$

Burgers later presented it as a mathematical model for turbulent flow.

It is a model for testing various numerical approaches, because it contains an advection term, UU_x, and a viscosity term, VU_{xx}. The Navier-Stokes equation in the one-dimensional version gives Burger's equation when the pressure and force variables are neglected [34]. The dimensional inhomogeneous fractional Burgers equation is a form of the classical Burgers equation that includes fractional derivatives and inhomogeneous variables [34]. This equation is also helpful since it allows us to compare the quality of numerical methods used to solve a non-linear problem. Researchers are working on Burger's equation, some of their studies with different numerical techniques include NHATM [17], DTM [34], MRPSM [35], VIM and ADM [36], NIM [37], and GDTM [38].

Because of their various applications in daily life, researchers have been continuing their studies to find the solutions to the N-W-S and Burger equations [39–49]. However, the research workers have yet to use this proposed hybrid technique to study the solution of these well-known equations. Motivated by the existing literature's gaps, the present research is the first of its kind to employ TPDTM to get the numerical approximate solutions for the N-W-S and Burger's equations.

The outline of the paper is as follows. Section 2 introduces specific terminology and mathematical foundations of the fractional calculus theory. In Section 3, the efficacy of the suggested approach is tested through the solution of N-W-S and Burger equations with fractional order derivatives. Section 4 provides the numerical results and a discussion of the findings. The findings are described and summarized in the conclusions in Section 5.

2. Methodology

2.1 *Basic definitions*

This section introduces a systematic overview of some definitions pertaining to fractional derivatives.

Definition 1 [50] The Reimann-Liouville fractional integrals operator of order $\alpha > 0$ of the left and right sided are defined for any function $f(t) \in L_1(a,\ b)$, $\alpha > 0$ as:

$$\left(I_{a^+}^{\alpha} f\right)(t) = \frac{1}{\Gamma(\alpha)} \int_a^{\infty} (t-\tau)^{\alpha-1} f(\tau) \mathrm{d}\tau,\ t > \alpha.$$

$$\left(I_{b^-}^{\alpha} f\right)(t) = \frac{1}{\Gamma(\alpha)} \int_{-\infty}^{b} (\tau - t)^{\alpha-1} f(\tau) \mathrm{d}\tau,\ t < \alpha.$$

Definition 2 [50] The Riemann integral on the half axis subjected to variable limit can be defined as

$$\left(I_{0^+}^{\alpha} f\right)(t) = \frac{1}{\Gamma(\alpha)} \int_a^{\infty} (t-\tau)^{\alpha-1} f(\tau) \mathrm{d}\tau,\ 0 < t < \infty.$$

Definition 3 [50] The left- and right-handed Riemann-Liouville fractional derivatives of order $\alpha,\ 0 < \alpha < 1$ in the interval $[a,\ b]$ are defined as

$$\left(D_{a^+}^{\alpha} f\right)(t) = \frac{1}{\Gamma(1-\alpha)} \frac{\mathrm{d}}{\mathrm{d}t} \int_a^t (t-\tau)^{-\alpha} f(\tau) \mathrm{d}\tau.$$

$$\left(D_{b^-}^{\alpha} f\right)(t) = \frac{1}{\Gamma(1-\alpha)} \frac{\mathrm{d}}{\mathrm{d}t} \int_t^b (\tau - t)^{-\alpha} f(\tau) \mathrm{d}\tau.$$

Definition 4 [51] The fractional derivative of $f(t)$ in the Caputo sense is defined by

$$D^{\alpha} f(t) = \frac{1}{\Gamma(n-\alpha)} \int_0^t (t-\tau)^{n-\alpha-1} f^n(\tau) \mathrm{d}\tau.$$

for $n-1 < \alpha \leq n,\ n \in N,\ t > 0$.

Definition 5 [50] The Mittag-Leffler function which is the generalization of exponential function is defined as

$$E_{\alpha}(Z) = \sum_{n=0}^{\infty} \frac{Z^n}{\Gamma(n\alpha + 1)}.$$

where $\alpha \in C, R(\alpha) > 0$.

2.2 *Tarig transform*

The Tarig transform of a time domain function, $f(t)$ is defined as follows [26]:

$$T[f(t)] = \frac{1}{\vartheta}\int_0^{\infty} e^{\frac{-t}{\vartheta^2}} f(t)\mathrm{d}t,\ \vartheta \neq 0. \tag{1}$$

where ϑ is the frequency domain variable.

Let $f(t)$ and $g(t)$ are two functions in the time domain. Their frequency domain functions under the Tarig transform are $F(\vartheta)$ and $G(\vartheta)$ respectively. If $F(\vartheta)$ is the Tarig transform of $f(t)$ with order α, the Tarig transform of the fractional integral of $f(t)$ with order α [26] is:

$$T\left[\left(I_{0^+}^{\alpha} f\right)(t)\right] = \vartheta^{2\alpha} F(\vartheta) = \vartheta^{2\alpha} T[f(t)]. \tag{2}$$

In a similar way, the Tarig transform of the fractional derivative of $f(t)$ of order α [25] is:

$$T[D^{\alpha} f(t)] = F^{\alpha}(\vartheta) = \frac{1}{\vartheta^{2\alpha}} F(\vartheta) - \sum_{i=1}^{n} \vartheta^{2(i-\alpha)-1} f^{(i-1)}(0). \tag{3}$$

2.3 *Projected differential transform method (PDTM)*

I. If $f(r_1, r_2, \ldots, r_n)$ is a multivariable function, its PDTM can be defined [27] as follows:

$$f(r_1, r_2, \ldots, r_{n-1}, k) = \frac{1}{k!}\left[\frac{\partial^k f(r_1, r_2, \ldots, r_n)}{\partial r_n^k}\right]_{r_n}. \tag{4}$$

where $f(r_1, r_2, \ldots, r_n)$ is the original function, while the projected differential transform function is $f(r_1, r_2, \ldots, r_{n-1}, k)$.

II. The differential inverse transform of $f(r_1, r_2, \ldots, r_{n-1}, k)$ can be defined [27] as follows:

$$f(r_1, r_2, \ldots, r_n) = \sum_{k=0}^{\infty} f(r_1, r_2, \ldots, r_{n-1}, k)(r - r_0)^k. \tag{5}$$

Now, we will give some fundamental theorems obtained by the PDTM that are pertinent to our work.

III. Let $u(r_1, r_2, \ldots, r_n)$ and $v(r_1, r_2, \ldots, r_n)$ be any two multivariable functions and their transformed functions are $u(r_1, r_2, \ldots, r_{n-1}, k)$ and $v(r_1, r_2, \ldots, r_{n-1}, k)$ respectively. Let c be a constant. If [27],

i. $z(r_1, r_2, \ldots, r_n) = u(r_1, r_2, \ldots, r_n) \pm v(r_1, r_2, \ldots, r_n)$, then $z(r_1, r_2, \ldots, r_{n-1}, k) = u(r_1, r_2, \ldots, r_{n-1}, k) \pm v(r_1, r_2, \ldots, r_{n-1}, k)$.

ii. $z(r_1, r_2, \ldots, r_n) = cu(r_1, r_2, \ldots, r_n)$, then, $z(r_1, r_2, \ldots, r_{n-1}, k) = cu(r_1, r_2, \ldots, r_{n-1}, k)$.

iii. $z(r_1, r_2, \ldots, r_n) = \dfrac{d^n u(r_1, r_2, \ldots, r_n)}{dr_n^n}$, then, $z(r_1, r_2, \ldots, r_{n-1}, k) = \dfrac{k+n}{k!} u(r_1, r_2, \ldots, r_{n-1}, k+n)$.

iv. $z(r_1, r_2, \ldots, r_n) = u(r_1, r_2, \ldots, r_n) v(r_1, r_2, \ldots, r_n)$, then $z(r_1, r_2, \ldots, r_{n-1}, k) = \sum_{m=0}^{k} u(r_1, r_2, \ldots, r_{n-1}, m)\, v(r_1, r_2, \ldots, r_{n-1}, m)$.

v. $z(r_1, r_2, \ldots, r_n) = u_1(r_1, r_2, \ldots, r_n) u_2(r_1, r_2, \ldots, r_n) \ \ldots\ u_n(r_1, r_2, \ldots, r_n)$, then $z(r_1, r_2, \ldots, r_{n-1}, k) = \sum_{k_{n-1}=0}^{k} \sum_{k_{n-2}=0}^{k_{n-1}} \ldots \sum_{k_2=0}^{k_3} \sum_{k_1=0}^{k_2} u_1(r_1, r_2, \ldots, r_{n-1}, k_1) u_2(r_1, r_2, \ldots, r_{n-1}, k_2 - k_1)\, u_{n-1}(r_1, r_2, \ldots, r_{n-1}, k_{n-1} - k_{n-2}) \ldots u_n(r_1, r_2, \ldots, r_{n-1}, k - k_{n-1})$.

2.4 *Basic algorithm of TPDTM*

Consider the given non-linear time-fractional PDE:

$$D^{\alpha}U(x,\,t)+RU(x,\,t)+NU(x,\,t)=g(x,\,t). \tag{6}$$

with the initial condition:

$$U(x,\,0)=f(x). \tag{7}$$

where $D^{\alpha}=\dfrac{\partial^{\alpha}}{\partial t^{\alpha}}$ is the fractional order differential operator, R is the linear differential operator, N is the non-linear differential operator and $g(x,\,t)$ is the source term.

By applying the Tarig transform (T) [25] on both sides of equation (6), we get

$$T\left[D^{\alpha}U(x,\,t)\right]+T\left[RU(x,\,t)\right]+T\left[NU(x,\,t)\right]=T\left[g(x,\,t)\right]. \tag{8}$$

Using the differential property of Tarig transform (3) [25] on equations (6) and (7), we get

$$T\left[U(x,\,t)\right]=\vartheta f(x)+\vartheta^{2\alpha}\left[T\left[g(x,\,t)\right]-T\left[RU(x,\,t)\right]+\,T\left[NU(x,\,t)\right]\right]. \tag{9}$$

Applying the inverse of the Tarig transform [25] on both sides of equation (9), we get,

$$U(x,\,t)=G(x,\,t)-T^{-1}\left[\vartheta^{2\alpha}\left[T\left[RU(x,\,t)\right]+\,T\left[NU(x,\,t)\right]\right]\right]. \tag{10}$$

where $G(x,\,t)$ represent the term arising from the source term and the initial condition.

Using PDTM [25], the non-linear term can be decomposed as

$$U(x,\,m+1)=-T^{-1}\left[\vartheta^{2\alpha}\left[T\left[RU(x,\,m)\right]+T\left[NU(x,\,m)\right]\right]\right],\ m\geq 0,\ U(x,\,0)=f(x). \tag{11}$$

The exact solution of equations (6) and (7) is of the series form:

$$U(x,\,t)=\sum_{m=0}^{\infty}U(x,\,m). \tag{12}$$

where $U(x,\,m)$ is obtained as a function of x and t.

2.5 *Error calculation, stability and convergence of the method*

It is important to understand the convergence of the series obtained in equation (12) by TPDTM. The approximate solution of the equation (6) with the initial condition (7) can be obtained as

$$U_{\text{app}(k)}(x,\ t) = \sum_{m=0}^{k} U(x,\ m).$$

From equation (12) by shortening the terms for $m = k+1,\ k+2, \ldots \infty$. Then, the exact solution of equation (6) with equation (7) is represented as

$$U(x,\ t) = U_{\text{app}(k)}(x,\ t) + eU_k(x,\ t).$$

where $eU_k(x,\ t)$ is the error function.

Generally, the absolute error is defined as $eU_k(x,\ t) = \left|U(x,\ t) - U_{\text{app}(k)}(x,\ t)\right|$. But in most real-world cases the exact solution $U(x,\ t)$ is unknown. So, define the approximate absolute error as

$$EU_k(x,\ t) = \left|U_{\text{app}(k)}(x,\ t) - U_{\text{app}(k+1)}(x,\ t)\right|. \tag{13}$$

To conform the convergence of equation (12), it is essential to show that the sequence $\{EU_k(x,\ t)\}$ is a convergent sequence. Since the convergence is bounded below, it is sufficient to show that the sequence $\{EU_k(x,\ t)\}$ exhibits monotonic decreasing behavior.

Hence, the convergence criteria is $\left|\dfrac{EU_p(x,\ t)}{EU_k(x,\ t)}\right| < 1$, for $k < p$.

With the following algorithm, the convergence of the iterative solution $U_{\text{app}(k)}(x,\ t)$ to the exact solution $U(x,\ t)$ can be shown as follows [25].

• Determine $U_{\text{app}(k)}(x,\ t)$, $U_{\text{app}(k+1)}(x,\ t)$.

• Determine $U_{\text{app}(p)}(x,\ t)$, $U_{\text{app}(p+1)}(x,\ t)$, $k \leq p$.

• Define $EU_k(x,\ t) = \left|U_{\text{app}(k)}(x,\ t) - U_{\text{app}(k+1)}(x,\ t)\right|$, $EU_p(x,\ t) = \left|U_{\text{app}(p)}(x,\ t) - U_{\text{app}(p+1)}(x,\ t)\right|$, for some t and x.

• If $EU_k(x,\ t) \geq EU_p(x,\ t)$, it can be inferred that $U_{\text{app}(k)}(x,\ t)$ converges to the exact solution $U(x,\ t)$ when $k \to \infty$.

This approach is used in this study to demonstrate the convergence of the series solution found using TPDTM.

2.6 *Basic algorithm for FDM and LADM*

Algorithm for FDM [12, 52]

Step 1: Consider the PDE, specify the temporal and spatial domains and discretize them.

Step 2: Use the finite difference approximations and update the equation by combining these approximations.

Step 3: Use the boundary conditions and iteratively solve the resulting equations.

Step 4: Store the solution as $U(x,\ t)$.

Algorithm for LADM [15, 31]

Step 1: Consider the PDE, with initial conditions and then apply Laplace transform.

Step 2: The nonlinear term is broken down into Adomian polynomials.

Step 3: Iteratively solve the resulting equations.

Step 4: Apply inverse Laplace transform to get the approximate solution $U(x,\ t)$.

3. Numerical test examples

3.1 *Newell-whitehead-segel equation*

The N-W-S equation, $D^{\alpha}U = U_{xx} - 2U,\ 0 < \alpha \leq 1$, is obtained from the fractional N-W-S equation $D^{\alpha}U = kU_{xx} + aU - bU^{q},\ 0 < \alpha \leq 1,$ by putting $k = 1$, $a = -2$, and $b = 0$, and we omit the non-linear term q.

Consider the linear time fractional N-W-S equation

$$D^{\alpha}U = U_{xx} - 2U,\ 0 < \alpha \leq 1. \tag{14}$$

with initial condition

$$U(x,\ 0) = e^{x}. \tag{15}$$

If $\alpha = 1$, then the exact solution of equation (14) with initial condition (15) is e^{x-t}. Apply Tarig transform on RHS and LHS of the equation (14) and using the differential property of Tarig transform (3), we get

$$T\left[U(x,\ t)\right] = \vartheta e^{x} + \vartheta^{2\alpha}\left[T\left[U_{xx} - 2U\right]\right]. \tag{16}$$

Applying inverse Tarig transform on two sides of equation (16), we get

$$U(x,\ t) = e^{x} + T^{-1}\left[\vartheta^{2\alpha}\left[T\left[U_{xx} - 2U\right]\right]\right],\ \text{since } T^{-1}(\vartheta) = 1. \tag{17}$$

Using PDTM, equation (17) can be transformed to

$$U(x,\ m+1) = T^{-1}\left[\vartheta^{2\alpha}\left[T\left[U_{xx} - 2U\right]\right]\right],\ m \geq 0,\ U(x,\ 0) = e^{x}. \tag{18}$$

From the equation (18), we obtain:

$$U(x,\ 1) = -e^{x}\frac{t^{\alpha}}{\Gamma(\alpha+1)}.$$

$$U(x,\ 2) = e^{x}\frac{t^{2\alpha}}{\Gamma(2\alpha+1)}.$$

$$U(x,\ 3) = -e^{x}\frac{t^{3\alpha}}{\Gamma(3\alpha+1)}.$$

$$\ldots$$

$$U(x,\ n) = (-1)^n e^x \frac{t^{n\alpha}}{\Gamma(n\alpha+1)}.$$

We iteratively derive the remaining terms of the series in the same manner. Thus, utilizing the TPDTM, the series solution of the problem (14) with (15) is provided by

$$U(x,\ t) = U(x,\ 0) + U(x,\ 1) + U(x,\ 2) + \ldots = e^x \sum_{k=0}^{\infty} (-1)^k \frac{t^{k\alpha}}{\Gamma(k\alpha+1)}. \tag{19}$$

The recursive structure of the series solution (19) by using TPDTM, with each term is found by utilizing the fractional calculus formulation of the governing equation.

3.2 *Burger's equation*

In this paper, we consider the Burger's equation with zero viscosity

$$U_t + UU_x = 0. \tag{20}$$

which is also known as the inviscid Burger's equation. The classical study of inviscid Burger's equation is the base for studying more sophisticated non-linear wave equations, because it possesses non-linear conservation principles.

Consider the inviscid Burger's equation,

$$D^{\alpha}U = -UU_x,\ \text{with initial condition } U(x,\ 0) = x. \tag{21}$$

If $\alpha = 1$, then the exact solution of equation (21) is $\dfrac{x}{t+1}$.

Apply Tarig transform on LHS and RHS parts of the equation (20) and using the differential property of Tarig transform (3), we get

$$T\left[U(x,\ t)\right] = \vartheta x - \vartheta^{2\alpha}\left[T\left[UU_x\right]\right]. \tag{22}$$

Applying inverse Tarig transform on two sides of the equation (22), we get

$$U(x,\ t) = x - T^{-1}\left[\vartheta^{2\alpha}\left[T\left[UU_x\right]\right]\right],\ \text{since } T^{-1}(\vartheta) = 1. \tag{23}$$

Using PDTM, equation (23) transformed to

$$U(x,\ m+1) = -T^{-1}\left[\vartheta^{2\alpha}\left[T\left[UU_x\right]\right]\right],\ m \geq 0,\ U(x,\ 0) = x. \tag{24}$$

From the equation (24), we obtain:

$$U(x,\ 1) = \frac{-x}{\Gamma(\alpha+1)}t^{\alpha}$$

$$U(x,\ 2) = \frac{-x}{(\Gamma(\alpha+1))^{2}}\left(\frac{\Gamma(2\alpha+1)}{\Gamma(3\alpha+1)}\right)t^{3\alpha}$$

$$U(x,\ 3) = \frac{-x}{(\Gamma(\alpha+1))^{4}}\left(\frac{\Gamma(2\alpha+1)}{\Gamma(3\alpha+1)}\right)^{2}\left(\frac{\Gamma(4\alpha+1)}{\Gamma(5\alpha+1)}\right)t^{5\alpha}$$

$$U(x,\ 4) = \frac{-x}{(\Gamma(\alpha+1))^{8}}\left(\frac{\Gamma(2\alpha+1)}{\Gamma(3\alpha+1)}\right)^{4}\left(\frac{\Gamma(4\alpha+1)}{\Gamma(5\alpha+1)}\right)^{2}\left(\frac{\Gamma(6\alpha+1)}{\Gamma(7\alpha+1)}\right)t^{7\alpha}$$

$$\ldots$$

$$U(x,\ n) = \frac{-x}{(\Gamma(\alpha+1))^{(2n-2)}}\prod_{k=1}^{n}\left(\frac{\Gamma((2k)\alpha+1)}{\Gamma((2k+1)\alpha+1)}\right)^{2^{n-k}}t^{(2n-1)\alpha}.$$

We iteratively derive the remaining terms of the series in the same manner. Thus, utilizing the TPDTM, the series solution of the problem (21) is provided by

$$U(x,\ t) = U(x,\ 0)+U(x,\ 1)+U(x,\ 2)+\ldots = x-\sum_{n=1}^{\infty}\frac{x}{(\Gamma(\alpha+1))^{(2n-2)}}\prod_{k=1}^{n}\left(\frac{\Gamma((2k)\alpha+1)}{\Gamma((2k+1)\alpha+1)}\right)^{2^{n-k}}t^{(2n-1)\alpha}. \quad (25)$$

The recursive structure of the series solution (25) by using TPDTM, with each term is found by utilizing the fractional calculus formulation of the governing equation.

4. Results and discussion

Approximate solutions of the time-fractional N-W-S and Burger equations were solved via TPDTM using MATLAB software. To understand the efficacy of TPDTM, a comparative analysis between TPDTM and FDM [12, 52] and LADM [15, 31] is made. Table 1 represents the approximate numerical solution of the fractional N-W-S equation for different values of fractional order $\alpha = 0.25,\ 0.50,\ 0.75,$ and 1. The corresponding graphical representations are shown in Figures 1 and 2. Figures 3-5 indicate the approximate numerical solution of the fractional N-W-S equation obtained by TPDTM, FDM, and LADM. From Figures 3 and 5, it is obvious that the solutions obtained exhibit uniformity using TPDTM (Figure 3) and LADM (Figure 5), though Figure 4 exhibits sharper gradients and variations near the boundary regions.

To quantitatively validate this observation, we compare the absolute error as:

$$\text{Absolute error} = |\ \text{Exact solution} - \text{TPDTM approximate solution}|.$$

and the relative error as:

$$\text{Relative error} = \frac{|\text{ Exact solution} - \text{TPDTM approximate solution }|}{|\text{ Exact solution }|}.$$

for different values of k and x. The results show a decreasing error trend, reinforcing the convergence of TPDTM.

Table 1. Numerical values of $U(x, t)$ for different values of α and x for a fixed value of t of test example 1

x	$U(x, t)$ at $t = 1$			
	$\alpha = 0.25$	$\alpha = 0.5$	$\alpha = 0.75$	$\alpha = 1$
−5	0.0031254	0.002881	0.0026487	0.0024788
−4	0.0084958	0.0078315	0.0072	0.0067379
−3	0.023094	0.021288	0.019572	0.018316
−2	0.062776	0.057867	0.053201	0.049787
−1	0.17064	0.1573	0.14462	0.13534
0	0.46385	0.42758	0.39311	0.36788
1	1.2609	1.1623	1.0686	1
2	3.4274	3.1594	2.9047	2.7183
3	9.3167	8.5882	7.8958	7.3891
4	25.326	23.345	21.463	20.086
5	68.842	63.459	58.342	54.598

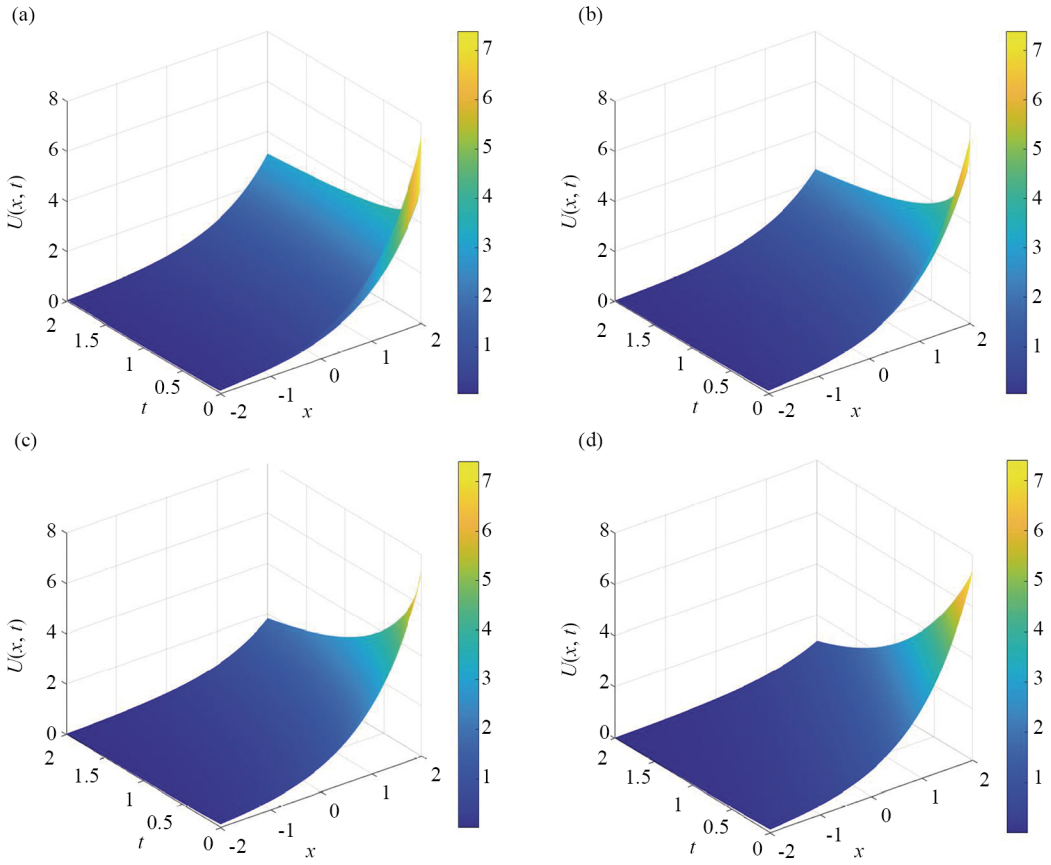

Figure 1. The approximate solution $U(x, t)$ for different values (a) $\alpha = 0.25$, (b) $\alpha = 0.50$, (c) $\alpha = 0.75$, and (d) $\alpha = 1$ of test example 1

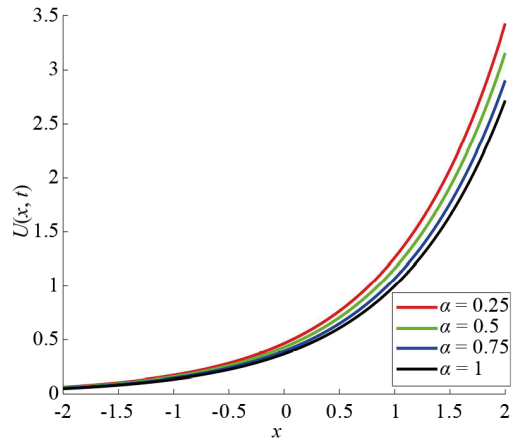

Figure 2. Plots of $U(x,\ t)$ vs. x at $\alpha = 0.25,\ 0.5,\ 0.75$, and $\alpha = 1$ at $t = 1$ for approximate solution of test example 1

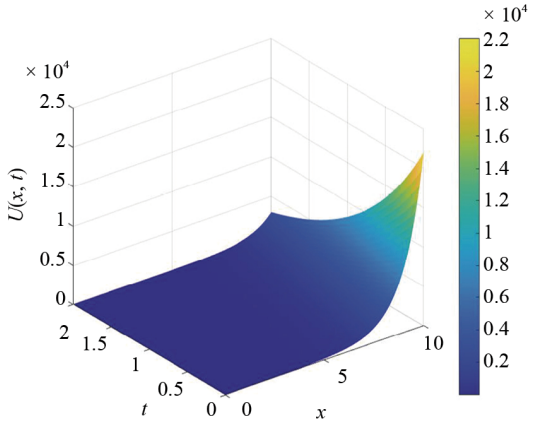

Figure 3. Plots of $U(x,\ t)$ for $\alpha = 1$ using TPDTM for test example 1

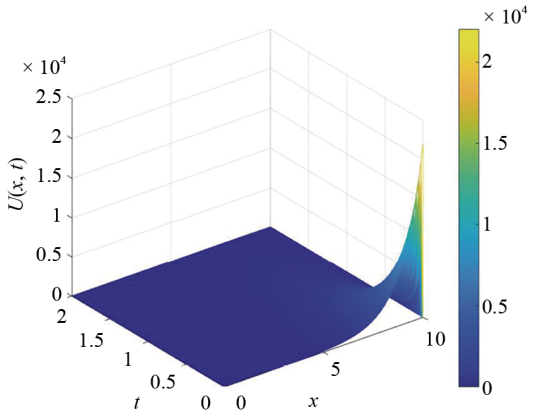

Figure 4. Plots of $U(x,\ t)$ for $\alpha = 1$ using FDM for test example 1

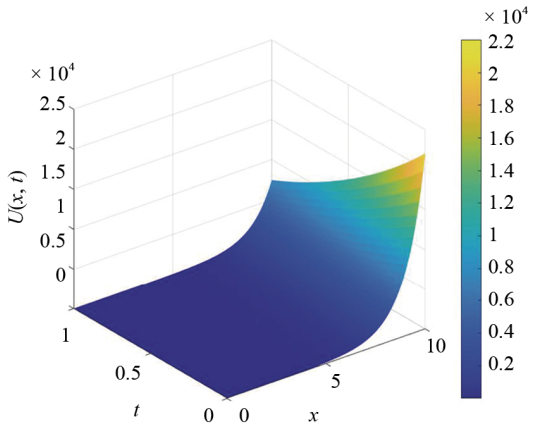

Figure 5. Plots of $U(x, t)$ for $\alpha = 1$ using LADM for test example 1

To compare TPDTM with other methods, such as the Adomian Decomposition Method (ADM) or Homotopy Perturbation Method (HPM), we observe that TPDTM yields lower absolute and relative errors for the same number of terms. This indicates that TPDTM provides better convergence efficiency while maintaining stability. Therefore, based on the error analysis and comparative results, it can be concluded that TPDTM is an effective, accurate, and stable method for solving the N-W-S equation.

From Figure 6, the exact and approximate solutions of the fractional N-W-S equation obtained using TPDTM exhibit perfect agreement. Additionally, Table 2 presents the maximum errors for each k at various x-values, offering deeper insight into the stability and convergence characteristics of TPDTM. Using equation (13), the absolute approximate solution of the N-W-S equation is tabulated in Table 2. From Table 2, it is observed that an increase in k results in a reduction in the value of error, demonstrating the approximate solution obtained using the TPDTM method converges toward the exact solution, which indicates the method TPDTM converging well. Furthermore, the error remains stable without rapid growth. It can, therefore, be concluded that TPDTM provides a reliable and stable numerical approach.

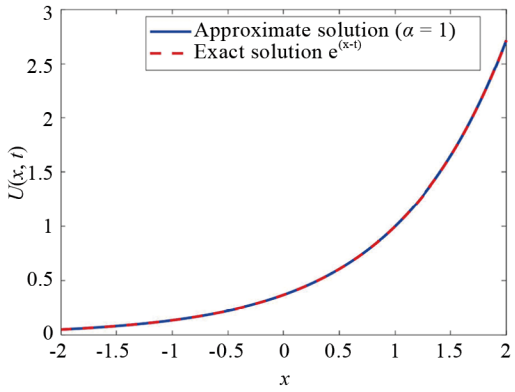

Figure 6. Comparison between exact and approximate solutions when $\alpha = 1$ of test example 1

Table 2. Absolute error calculation of approximate solution of $U(x, t)$ for different values of x with $t = 1$ of test example 1

k	x values					
	1	2	4	6	8	10
1	2.7183	7.3891	54.598	403.43	2,981	22,026
2	1.3591	3.6945	27.299	201.71	1,490.5	11,013
3	0.45305	1.2315	9.0997	67.238	496.83	3,671.1
4	0.11326	0.30788	2.2749	16.81	124.21	917.77
5	0.022652	0.061575	0.45498	3.3619	24.841	183.55
6	0.0037754	0.010263	0.075831	0.56032	4.1402	30.592
7	0.00053934	0.0014661	0.010833	0.080045	0.59146	4.3703
8	6.7418e-05	0.00018326	0.0013541	0.010006	0.073932	0.54629
9	7.4909e-06	2.0362e-05	0.00015046	0.0011117	0.0082147	0.060699

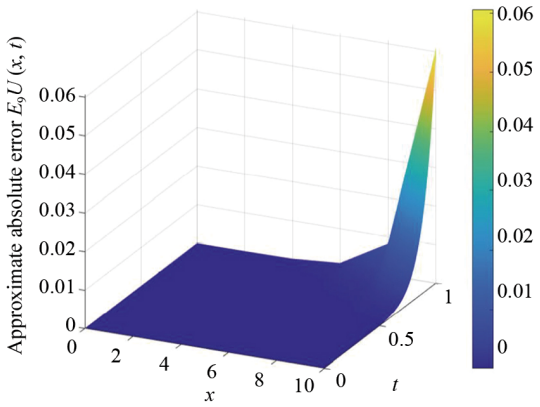

Figure 7. Absolute error $E_9U(x, t) = |\text{Exact} - \text{Approximate value}|$ of test example 1

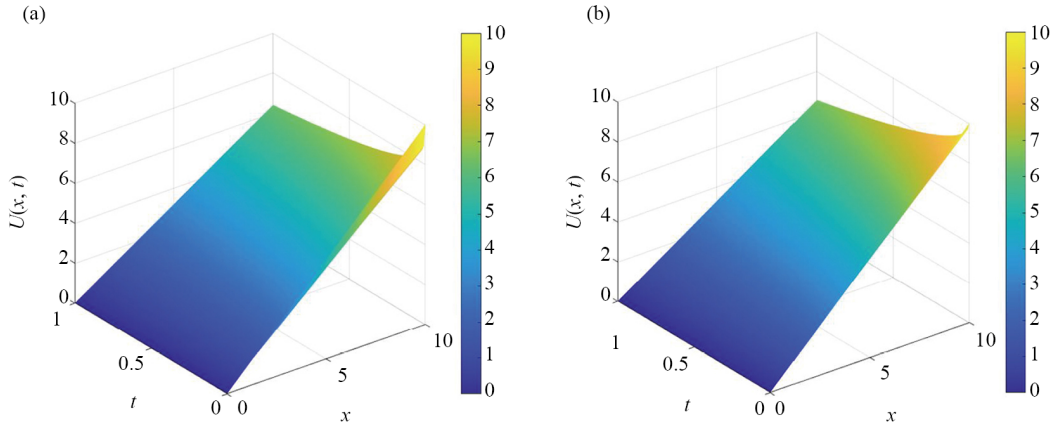

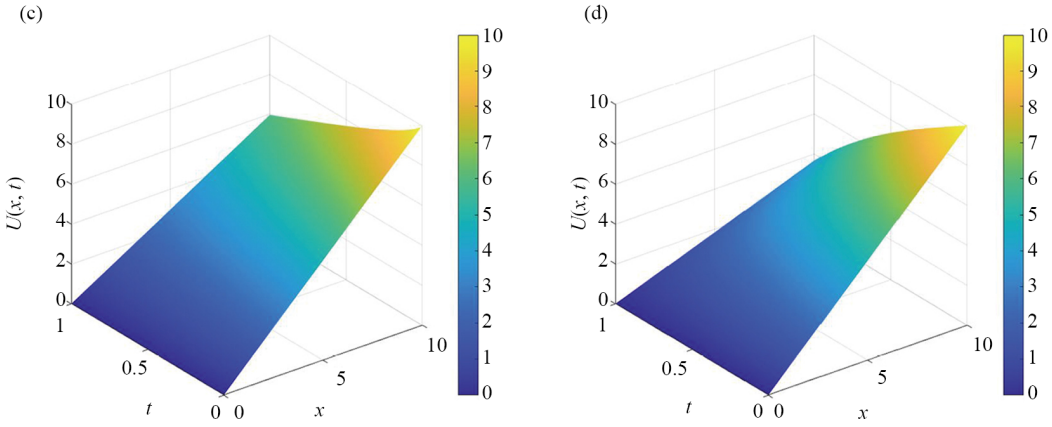

Figure 8. The approximate solution $U(x, t)$ for different values of α (a) $\alpha = 0.25$, (b) $\alpha = 0.50$, (c) $\alpha = 0.75$, and (d) $\alpha = 1$ of test example 2

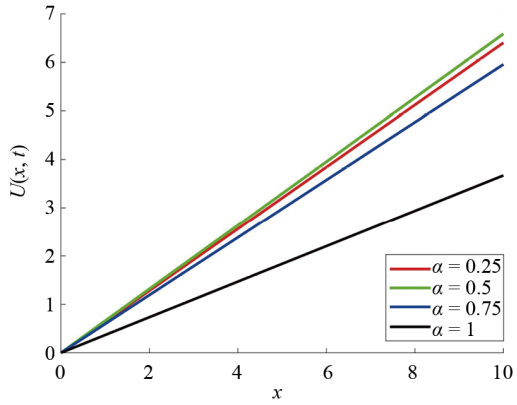

Figure 9. Plots of $U(x, t)$ vs. x at $\alpha = 0.25, 0.5, 0.75$, and $\alpha = 1$ at $t = 1$ for approximate solution using TPDTM of test example 2

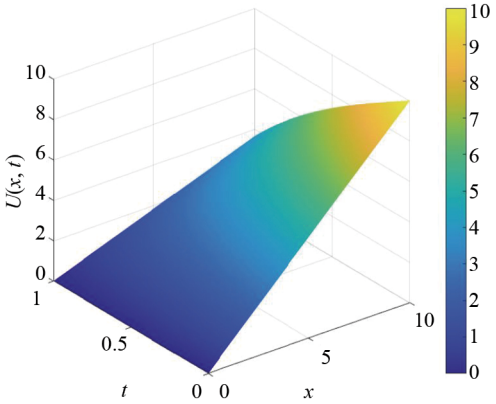

Figure 10. Plots of $U(x, t)$ for $\alpha = 1$ using TPDTM for test example 2

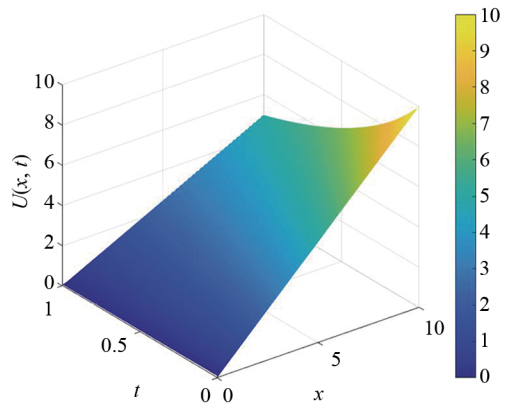

Figure 11. Plots of $U(x, t)$ for $\alpha = 1$ using FDM for test example 2

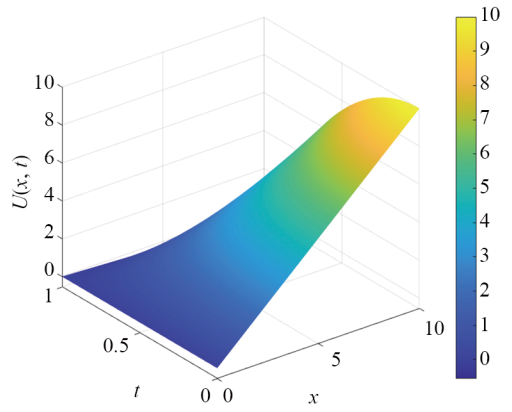

Figure 12. Plots of $U(x, t)$ for $\alpha = 1$ using LADM for test example 2

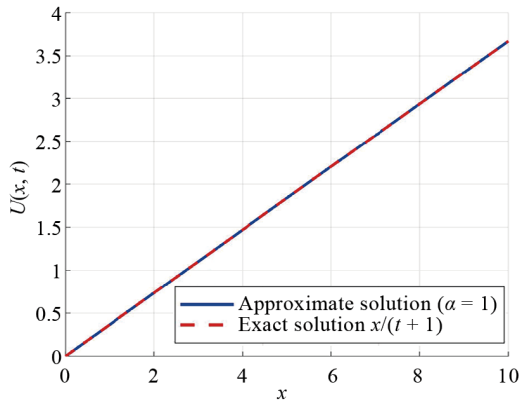

Figure 13. Comparison between exact and approximate solutions when $\alpha = 1$ of test example 2

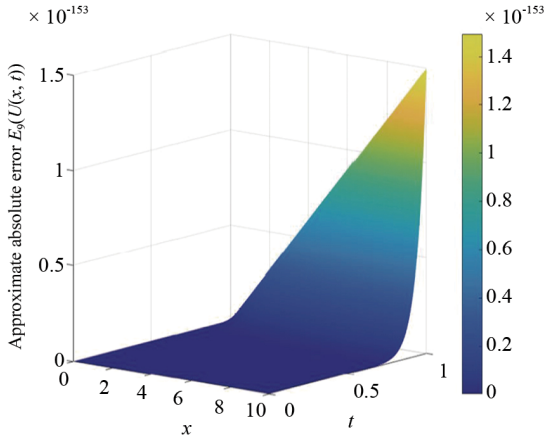

Figure 14. Absolute error $E_9U(x,\ t) = |\text{Exact} - \text{Approximate value}|$ of test example 2

Figure 7 gives the absolute error of ninth term of the series. By increasing the number of iterations, it is possible to increase the accuracy of the method. Table 3 represents the approximate numerical solution of the fractional Burger equation for different values of fractional order $\alpha = 0.25,\ 0.50,\ 0.75,\ 1$, and the graphical representation of Table 3 is depicted in Figures 8 and 9. Figures 10-12 indicate the approximate numerical solution of fractional Burger's equation obtained by TPDTM, FDM, and LADM. From Figures 10-13, it is clear that there is a uniformity between solutions obtained using TPDTM (Figure 10) and LADM (Figure 12). From Figure 14, it is clear that the exact and approximate solution of the fractional Burger equation using TPDTM are in complete agreement at $\alpha = 1$. The maximum errors for each k for different values of x are listed in Table 4, providing a better understanding of the stability and convergence of the numerical method.

Table 3. Numerical values of $U(x,\ t)$ for different values of α and x for fixed value of t of test example 2

x	$U(x,\ t)$ at $t = 1$			
	$\alpha = 0.25$	$\alpha = 0.5$	$\alpha = 0.75$	$\alpha = 1$
−5	−3.2021	−3.294	−2.9788	−1.8358
−4	−2.5616	−2.6352	−2.3831	−1.4686
−3	1.9212	−1.9764	−1.7873	−1.1015
−2	−1.2808	−1.3176	−1.1915	−0.73431
−1	−0.64041	−0.65881	−0.59577	−0.36716
0	0	0	0	0
1	0.64041	0.65881	0.59577	0.36716
2	1.2808	1.3176	1.1915	0.73431
3	1.9212	1.9764	1.7873	1.1015
4	2.5616	2.6352	2.3831	1.4686
5	3.2021	3.294	2.9788	1.8358

Using equation (13), the absolute approximate solution of Burgers equation is tabulated in Table 4. Table 4, an increase in k results in a reduction in the value of error demonstrates that the approximate solution using TPDTM approaches to the exact solution. Therefore, the present method (TPDTM) converges well. It is also evident from the analysis that the error remains constant and there is no rapid growth, implying that the TPDTM is stable. Figure 14 gives

the absolute error of the ninth term of the series. By increasing the number of iterations, one can increase the accuracy of the method.

Table 4. Absolute error calculation of approximate solution of $U(x, t)$ for different value of x with $t = 1$ of test example 2

k	x values					
	0	2	4	6	8	10
1	0	0.75	1.5	2.25	3	3.75
2	0	0.23438	0.46875	0.70312	0.9375	1.1719
3	0	0.015564	0.031128	0.046692	0.062256	0.07782
4	0	6.1034e-05	0.00012207	0.0001831	0.00024414	0.00030517
5	0	9.3132e-10	1.8626e-09	2.794e-09	3.7253e-09	4.6566e-09
6	0	2.1684e-19	4.3368e-19	6.5052e-19	8.6736e-19	1.0842e-18
7	0	1.1755e-38	2.351e-38	3.5265e-38	4.702e-38	5.8775e-38
8	0	3.4545e-77	6.9089e-77	1.0363e-76	1.3818e-76	1.7272e-76
9	0	2.9833e-154	5.9667e-154	8.95e-154	1.1933e-153	1.4917e-153

It may be worth mentioning that in all figures, higher values of $U(x, t)$ is represented by a yellow colour, whereas the lower value is represented by a blue colour. Figures 1a-d and 8a-d show the spatial and temporal diffusion of the solution $U(x, t)$ with varying values of α. Figures 2 and 9 show spatial diffusion of the solution $U(x, t)$ for a constant time $t = 1$ with varying values of α of example 1 and 2 in three dimensions and two dimensions, respectively. Memory effects are introduced by the fractional time derivative D^{α}, when $0 < \alpha < 1$, which is frequently seen in systems with anomalous diffusion or non-classical dynamics [53].

From Figures 1a-d and 2, for a given x, the solution $U(x, t)$ shows a noticeable rise in magnitude as α drops from 1 to 0.25. This illustrates how the dynamics are affected by the memory effect, which is controlled by D^{α}. Because of the slower temporal decay caused by smaller α values, $U(x, t)$ might expand more dramatically. The absence of memory effects causes the solution to decay more quickly if $\alpha = 1$, as seen in Figures 2 and 3. It is evident from Figure 8a-d that the slope of $U(x, t)$ steepens with increasing α, indicating larger nonlinear effects. Figure 9 illustrates the nonlinear character of the Burgers equation by showing how changing α impacts the wave propagation and steeping rate.

Figures 3 and 5 illustrate the smooth evolution of $U(x, t)$, while Figures 10 and 12 confirm the stability of the solution for the N-W-S and Burgers equations through TPDTM and LADM. Figure 4 shows a sharp rise in $U(x, t)$ at high x and low t, suggesting instability from the nonlinear interaction of diffusion and reaction terms. Figures 1-5 show $U(x, t)$ peaks at larger x and low t, while lower values appear at smaller x and larger t.

The steep gradient in Figure 11 indicates that if the simulation is prolonged, a potential shock may occur. It is quite obvious that the FDM approach struggles to yield a smooth solution compared to TPDTM and LADM, as can be observed from Figures 4 and 11. The discrepancies between the computed data and the exact solution may stem from inherent discretization errors influenced by grid resolution, refinement of initial and boundary conditions, time step size, and grid spacing. Additionally, as the step size is directly proportional to the method's order, truncation errors arise when series expansions-fundamental to finite difference approximations-are truncated. These factors collectively contribute to the observed deviations.

Table 5 provides a comparative study between the present method and the existing method (FDM and LADM) for solving N-W-S and Burgers equations. Additionally, we carried out an analysis of the advantages of present methods with other numerical methods such as FEM [11], ADM [7], VIM [28, 38], HPM [8], HAM [18], etc. From this analysis, it is understood that high nonlinearities are handled efficiently by TPDTM without the aid of linearization, perturbation, or Adomian polynomials. TPDTM efficiently solves linear and nonlinear fractional differential equations with rapid convergence, bypassing mesh generation (FEM) and complex expansions (ADM). Unlike FDM, VIM, or LADM, it

minimizes fractional derivative errors without Laplace inversions. Free from auxiliary parameters or homotopy constructs (HPM and HAM), it ensures simplicity, reliability, and ease of implementation.

Table 5. Comparisons between the present method and existing methods (FDM and LADM)

The equation based on the study	Results from the literature		Present study
N-W-S equation	In this study, the time-spatial fractional N-W-S equations are solved using both standard and non-standard FDM (SFDM and NSFDM, respectively). They concluded that the proposed methods are conditionally stable and efficient [52].	In this study, LADM was used to solve the N-W-S equation. It concluded that this method is efficient and can be used to solve both linear and non-linear equations [31].	The numerical approximate solution using TPDTM is in good agreement with the exact solution. From the results, TPDTM is a simple approach, yet it has a high effectiveness and accuracy precision of results. Therefore, it may be concluded that TPDTM is an effective and yet easy to implement-reliable-computationally powerful method and attractive over the existing well-known methods.
Burger's equation	This study compares FDM and FEM for solving Burger's equation, concluding that finite element schemes are less economical due to the integral construction of algebraic formulas. The five-point finite difference method is the most efficient for steady solutions and fine mesh in the modified one-dimensional Burger's equation [12].	In this study, they used to solve the modified LADM. They concluded that this approach is straightforward and provides Burgers equation's analytical solution [15].	

5. Conclusions

The salient features of the present research are:

(a) The TPDTM-derived numerical approximation aligns remarkably well with the exact solution, demonstrating both high accuracy and computational efficiency.

(b) Despite its simplicity, TPDTM proves to be a powerful and precise method.

(c) The rapid convergence of approximate solutions for time-fractional N-W-S and Burgers equations further validates its robustness and reliability.

(d) Unlike conventional methods, TPDTM operates without the need for linearization, perturbation, discretization, or restrictive assumptions, making it a seamless and computationally efficient alternative.

(e) It's lower computational cost and ease of implementation position it as a superior choice over existing techniques.

(f) These research findings reinforce that TPDTM is not merely a theoretical construct but a valuable computational technique with significant real-world applicability.

As far as the future studies are concerned:

(a) TPDTM's versatility reaches beyond standard applications, offering promise for tackling higher-dimensional fractional equations, intricate boundary conditions, and complex phenomena in heat transfer and wave dynamics.

(b) The fusion of TPDTM with machine learning [54] could revolutionize its adaptability for nonlinear systems, while integration with multi-scale and multi-physics frameworks may pave the way for solving real-world engineering and scientific challenges.

(c) Future advancements will prioritize refining computational efficiency and validating theoretical results through experimental data, further solidifying TPDTM's role as a practical and impactful tool in applied research.

(d) Expanding TPDTM's applicability to coupled fractional systems and multi-scale problems will not only enhance its theoretical depth but also unlock new frontiers in engineering, physics, and computational modeling.

Acknowledgement

The authors would like to acknowledge the University Grant Commission (UGC), New Delhi, India, through the Savitribai Jyotirao Phule Fellowship for Single Girl Child (SJSGC) [F. No.82-7/2022 (SA-III)].

Statements and declarations

Since no new data were generated for this investigation, no data were linked to the paper.

Conflict of interest

The authors declare no conflict of interest.

References

[1] Khodadoost S, Saraee M, Talatahari S, Sareh P. Optimal design of fractional-order proportional integral derivative controllers for structural vibration suppression. *Scientific Reports*. 2024; 14(1): 17207. Available from: https://doi.org/10.1038/s41598-024-68281-2.

[2] Patel N, Patel H. Thermo-diffusion effects on fractional ordered model of unsteady casson blood flow with magnetic field effect. *Contemporary Mathematics*. 2025; 6(1): 1288-1306. Available from: https://doi.org/10.37256/cm.6120252609.

[3] Ozkan A, Ozkan EM. A novel study of analytical solutions of some important nonlinear fractional differential equations in fluid dynamics. *Modern Physics Letters B*. 2024; 39(11): 2450461. Available from: https://doi.org/10.1142/S021798492450461X.

[4] Owolabi KM, Jain S, Pindza E, Mare E. Comprehensive numerical analysis of time-fractional reaction-diffusion models with applications to chemical and biological phenomena. *Mathematics*. 2024; 12(20): 3251. Available from: https://doi.org/10.3390/math12203251.

[5] Kilbas AA, Srivastava HM, Trujillo JJ. *Theory and Applications of Fractional Differential Equations*. Amsterdam, Netherlands: Elsevier Science B. V; 2006.

[6] Baleanu D, Diethelm K, Scalas E, Trujillo JJ. *Fractional Calculus: Models and Numerical Methods*. Singapore: World Scientific; 2012.

[7] Prakash A, Verma V. Numerical method for fractional model of Newell-Whitehead-Segel equation. *Frontiers in Physics*. 2019; 7: 15. Available from: https://doi.org/10.3389/fphy.2019.00015.

[8] Mahgoub MMA. Homotopy perturbation method for solving-Whitehead-Segel equation. *Advances in Theoretical and Applied Mathematics*. 2016; 11(4): 399-406.

[9] Derakhshan M, Aminataei A. Homotopy perturbation transform method for time-fractional Newell-Whitehead Segel equation containing Caputo-Prabhakar fractional derivative. *AUT Journal of Mathematics and Computing*. 2020; 1(2): 235-250. Available from: https://doi.org/10.22060/ajmc.2020.18012.1028.

[10] Ahmad JA, Bibi ZE, Noor KA. Laplace decomposition method using He's polynomial to Burger's equation. *Journal of Science and Arts*. 2014; 14(2): 131-138.

[11] Devipriya G, Priya M. Galerkin finite element method for solving Newell-Whitehead-Segel equation. *Asia Mathematika*. 2019; 3(3): 41-47.

[12] Fletcher CA. A comparison of finite element and finite difference solutions of the one-and two-dimensional Burger's equations. *Journal of Computational Physics*. 1983; 51(1): 159-188.

[13] Prakash A, Kumar M. He's variational iteration method for the solution of nonlinear Newell-Whitehead-Segel equation. *Journal of Applied Analysis and Computation*. 2016; 6(3): 738-748. Available from: https://doi.org/10.11948/2016048.

[14] Patade J, Bhalekar S. Approximate analytical solutions of Newell-Whitehead-Segel equation using a new iterative method. *World Journal of Modelling and Simulation*. 2015; 11(2): 94-103.

[15] Naghipour A, Manafian J. Application of the Laplace Adomian decomposition and implicit methods for solving Burgers' equation. *TWMS Journal of Pure and Applied Mathematics*. 2015; 6(1): 68-77.

[16] Akinlabi GO, Edeki SO. Perturbation iteration transform method for the solution of Newell-Whitehead-Segel model equation. *arXiv:170306745*. 2017. Available from: https://arxiv.org/abs/1703.06745 [Accessed 7th March 2017].

[17] Kumar S, Kumar D. Fractional modelling for BBM-Burger equation by using new homotopy analysis transform method. *Journal of the Association of Arab Universities for Basic and Applied Sciences*. 2014; 16(1): 16-20. Available from: https://doi.org/10.1016/j.jaubas.2013.10.002.

[18] Song L, Zhang H. Application of homotopy analysis method to fractional KdV-Burgers-Kuramoto equation. *Physics Letters A*. 2007; 367(1-2): 88-94. Available from: https://doi.org/10.1016/j.physleta.2007.02.083.

[19] Zhou MX, Kanth AR, Aruna K, Raghavendar K, Rezazadeh H, Inc M, et al. Numerical solutions of time fractional Zakharov-Kuznetsov equation via Natural Transform Decomposition method with non-singular kernel derivatives. *Journal of Function Spaces*. 2021; 2021(1): 9884027. Available from: https://doi.org/10.1155/2021/9884027.

[20] Ravi Kanth AS, Aruna K, Raghavendar K. Natural transform decomposition method for the numerical treatment of the time fractional Burgers-Huxley equation. *Numerical Methods for Partial Differential Equations*. 2023; 39(3): 2690-2718. Available from: https://doi.org/10.1002/num.22983.

[21] Aruna K, Okposo NI, Raghavendar K, Inc M. Analytical solutions for the Noyes Field model of the time fractional Belousov Zhabotinsky reaction using a hybrid integral transform technique. *Scientific Reports*. 2024; 14(1): 25015. Available from: https://doi.org/10.1038/s41598-024-74072-6.

[22] Pavani K, Raghavendar K, Aruna K. Solitary wave solutions of the time fractional Benjamin Bona Mahony Burger equation. *Scientific Reports*. 2024; 14(1): 14596. Available from: https://doi.org/10.1038/s41598-024-65471-w.

[23] Singh J, Jassim HK, Kumar D, Dubey VP. Fractal dynamics and computational analysis of local fractional Poisson equations arising in electro statistics. *Communications in Theoretical Physics*. 2023; 75(12): 125002. Available from: https://doi.org/10.1088/1572-9494/ad01ad.

[24] Cui P, Jassim HK. Local fractional Sumudu decomposition method to solve fractal PDEs arising in mathematical physics. *Fractals*. 2024; 32(4): 1-7. Available from: https://doi.org/10.1142/S0218348X24400292.

[25] Bagyalakshmi M, SaiSundarakrishnan G. Tarig projected differential transform method to solve fractional nonlinear partial differential equations. *Boletim da Sociedade Paranaense de Matemática*. 2020; 38(3): 23-46. Available from: https://doi.org/10.5269/bspm.v38i3.34432.

[26] Elzaki TM, Elzaki SM. The new integral transform "Tarig Transform" properties and applications to differential equations. *Elixir International Journal*. 2011; 38: 4239-4242.

[27] Jang B. Solving linear and nonlinear initial value problems by the projected differential transform method. *Computer Physics Communications*. 2010; 181(5): 848-854. Available from: https://doi.org/10.1016/j.cpc.2009.12.020.

[28] Prakash A, Goyal M, Gupta S. Fractional variational iteration method for solving time-fractional Newell-Whitehead-Segel equation. *Nonlinear Engineering*. 2019; 8(1): 164-171. Available from: https://doi.org/10.1515/nleng-2018-0001.

[29] Aydin E, Cilingir Sungu I. On the efficient method for the fractional nonlinear Newell-Whitehead-Segel equations. *Computational Methods for Differential Equations*. 2024; 13(1): 95-106. Available from: https://doi.org/10.22034/CMDE.2024.58461.2472.

[30] Atta AG, Abd Elhameed WM, Youssri YH. Approximate collocation solution for the time fractional Newell-Whitehead-Segel equation. *Journal of Applied and Computational Mechanics*. 2024; 11(2): 529-540. Available from: https://doi.org/10.22055/jacm.2024.47269.4686.

[31] Pue-On P. Laplace Adomian decomposition method for solving Newell-Whitehead-Segel equation. *Applied Mathematical Sciences*. 2013; 7(132): 6593-6600. Available from: https://doi.org/10.12988/ams.2013.310603.

[32] Abdolmaleki E, Saberi Najafi H. Analytical solution for the time fractional Newell-Whitehead-Segel equation by using Modified Residual Power Series method. *International Journal of Nonlinear Analysis and Applications*. 2019; 10.

[33] Kumar NK. A review on Burger's equations and its applications. *Journal of Institute of Science and Technology*. 2023; 28(2): 49-52. Available from: https://doi.org/10.3126/jist.v28i2.61073.

[34] Abaxari R, Borhanifar A. Numerical study of the solution of the Burgers and couples Burgers equations by a differential transformation method. *Computers and Mathematics with Applications*. 2010; 59(8): 2711-2722. Available from: https://doi.org/10.1016/j.camwa.2010.01.039.

[35] Zhang J, Wei Z, Yong L, Xiao Y. Analytical solution for the time fractional BBM-Burger equation by using Modified Residual Power Series method. *Complexity*. 2018; 2018(1): 2891373. Available from: https://doi.org/10.1155/2018/2891373.

[36] Safari M, Ganji DD, Moslemi M. Application of He's variational iteration method and Adomian's decomposition method to the fractional kdV-Burgers-Kuramoto equation. *Computers and Mathematics with Applications*. 2009; 58(11-12): 2091-2097. Available from: https://doi.org/10.1016/j.camwa.2009.03.043.

[37] El-Ajou A, Arqub OA, Momani S. Approximate analytical solution of the nonlinear fractional KdV-Burgers equation: a new iterative algorithm. *Journal of Computational Physics*. 2015; 293: 81-95. Available from: https://doi.org/10.1016/j.jcp.2014.08.004.

[38] Liu J, Hou G. Numerical solutions of the space and time fractional coupled Burgers equations by generalized differential transform method. *Applied Mathematics and Computation*. 2011; 217(16): 7001-7008. Available from: https://doi.org/10.1016/j.amc.2011.01.111.

[39] Bektas U, Anac H. A hybrid method to solve a fractional-order Newell-Whitehead-Segel equation. *Boundary Value Problems*. 2024; 2024(1): 38. Available from: https://doi.org/10.1186/s13661-023-01795-2.

[40] Pathak M, Bhatia R, Joshi P, Mittal RC. A numerical study of Newell-Whitehead-Segel equations using fourth order Cubic B-Spline collocation method. *Mathematics and Statistics*. 2024; 12(3): 270-282.

[41] Xin X, khan I, Ganie AH, Akgul A, Bonyah E, Fathima D, et al. Comparative study of fractional Newell-Whitehead-Segel equations using optimal auxiliary function method and a novel iterative approach. *AIP Advances*. 2024; 14(3): 035232. Available from: https://doi.org/10.1063/5.0200059.

[42] Phumichot S, Poochinapan K, Wongsaijai B. Time fractional nonlinear evolution of dynamic wave propagation using the Burgers' equation. *Journal of Applied Mathematics and Computing*. 2024; 70(5): 3987-4020. Available from: https://doi.org/10.1007/s12190-024-02100-9.

[43] Shyaman VP, Sreelakshmi A, Awasthi A. An implicit tailored finite point method for the Burgers equation: Leveraging the Cole-Hopf transformation. *Physica Scripta*. 2024; 99(7): 075283. Available from: https://doi.org/10.1088/1402-4896/ad56d8.

[44] Popovych DR, Bihlo A, Popovych RO. Generalized symmetries of Burgers equation. *arXiv:240602809*. 2024. Available from: https://doi.org/10.48550/arXiv.2406.02809 [Accessed 4th June 2024].

[45] Chen X, Zhang W, Wu Y. Discrete transparent boundary conditions for Burgers' equations. *Engineering*. 2024; 16(12): 423-437.

[46] Gebril E, EL-Azab MS, Sameeh M. Chebyshev collocation method for fractional Newell-Whitehead-Segel equation. *Alexandria Engineering Journal*. 2024; 87: 39-46. Available from: https://doi.org/10.1016/j.aej.2023.12.025.

[47] Iqbal S, Wang J. Utilizing an imaginative approach to examine a fractional Newell-Whitehead-Segel equation based on the method HPA. *Journal of Engineering Mathematics*. 2024; 148(1): 4. Available from: https://doi.org/10.1007/s10665-024-10381-z.

[48] Cundin L. Newell-Whitehead-Segel equation: An exact generalized solution. *arXiv:240901501*. 2024. Available from: https://doi.org/10.48550/arXiv.2409.01501.

[49] He X, Xiong H, Qi J, Sun Y. Wave dynamics in design: The role of nonlinear potential Burgers equation with variable coefficients. *Advances in Mathematical Physics*. 2024; 2024(1): 1378156. Available from: https://doi.org/10.1155/admp/1378156.

[50] Samko SG. *Fractional Integrals and Derivatives: Theory and Applications*. London, UK: Taylor & Francis; 1993.

[51] Caputo M. *Elasticitae Dissipazione*. Bologna, Italy: Zanichelli; 1969.

[52] Sungu IC, Aydin E. On the convergence and stability analysis of finite-difference methods for the fractional Newell-Whitehead-Segel equations. *Turkish Journal of Mathematics*. 2022; 46(7): 2806-2818.

[53] Suzuki JL, Gulian M, Zayernouri M, D'Elia M. Fractional modeling in action: A survey of nonlocal modes for subsurface transport, turbulent flows, and anomalous materials. *Journal of Peridynamics and Nonlocal Modeling*. 2023; 5(3): 392-459. Available from: https://doi.org/10.1007/s42102-022-00085-2.

[54] Kumar V, Tewari RP, Pandey R, Rawat A. Triboinformatic modeling of wear in total knee replacement implants using machine learning algorithms. *Journal of Materials and Engineering*. 2023; 1(3): 97-105.